Acta Astronautica 178 (2021) 233–240

Contents lists available at ScienceDirect

Acta Astronautica

journal homepage: www.elsevier.com/locate/actaastro

Research paper

Fast initial design of low-thrust multiple gravity-assist three-dimensional trajectories based on the Bezier shape-based method

Zichen Fan [a], Mingying Huo [a,*], Ji Qi [b], Naiming Qi [a]

[a] School of Astronautics, Harbin Institute of Technology, Harbin 150001, China
[b] Ming Hsieh Department of Electrical and Computer Engineering, University of Southern California, Los Angeles, CA, 90007, United States of America

ARTICLE INFO

Keywords:
Low-thrust spacecraft
Multiple gravity-assist
Bezier shape-based method
Deep space exploration
Trajectory design

ABSTRACT

In deep space exploration, the application of low-thrust propulsion technology and multiple gravity-assist technology will greatly improve the scope of spacecraft exploration but will significantly increase the difficulty of trajectory design. This study proposes a fast initial design method of low-thrust trajectories, which reasonably combines low-thrust propulsion and multiple gravity-assist technology. In this paper, the Bezier shape-based method is combined with the gravity-assist algorithm to obtain a fast algorithm for calculating the low-thrust multiple gravity-assist transfer trajectories. For the design of the Jupiter rendezvous trajectories, the feasibility of the proposed method is proved by comparing several calculation examples with and without gravity assistance. In order to prove the effectiveness of the proposed method, it is compared with the finite Fourier series (FFS) shape-based method. The simulation results show that the proposed method can use shorter computation time to obtain transfer trajectories with smaller velocity increments than the FFS shape-based method. In order to prove the superiority of the proposed method, the results obtained by the proposed method are used as initial values for further optimization of the Gauss pseudospectral method (GPM). The simulation results show that the difference between the performance indexes of the Bezier method and the GPM is only about 2%, while the Bezier method only uses approximately 2% of the computation time of the GPM. The method described in this paper is significant for obtaining a feasible initial solution quickly for a large number of design cases.

1. Introduction

The exploration of the solar system has attracted people's attention [1,2]. In some deep space exploration missions in the past, the low-thrust propulsion technology and the gravity-assist technology have played crucial roles and showed great advantages [3–7]. Deep Space 1 [8,9] was the first spacecraft to use an ion engine to complete interplanetary flight, while Voyager 2 [10] has used gravity-assist many times in its exploration of the solar system. The success of these deep space exploration missions display the superiority of these two technologies and the potential of their widespread application in the future. Therefore, the trajectory design for deep space missions with the combination of high-efficiency continuous-thrust propulsion and the multiple gravity-assist technology [11] has significant advantages, which provides a new method for conducting solar system missions [12–16]. However, the joint application of these two technologies greatly increases the complexity and difficulty of the initial trajectory design.

The design of low-thrust trajectory is usually transformed into the optimal control problem, which can be solved using the direct optimization algorithm or indirect optimization algorithm. And the GPM [17] is a direct optimization solver. However, these methods require an initial guess of their solution, which is challenging to obtain quickly, especially when the multi gravity-assist technology is introduced. For the low-thrust trajectory design, the shape-based method was first proposed by Petropoulos and Longuski [18]. Subsequently, a variety of shape-based methods have been proposed [19–27]. In 2012, Abdelkhalik and Taheri first proposed using the FFS method to describe the low-thrust trajectory [28]. This method can quickly generate the appropriate initial solution of the low-thrust trajectory [29–33]. Furthermore, Huo et al. [34] used the Bezier function to describe the electric sail transfer trajectory. In the above study, the Bezier shape-based method [34,35] and other shape-based methods [26–28] are usually applied to the problem of spacecraft interplanetary transfer trajectory generation. These methods assume the trajectory as the corresponding function shapes and limit them to satisfy the motion equation and boundary

* Corresponding author.
E-mail address: huomingying@hit.edu.cn (M. Huo).

https://doi.org/10.1016/j.actaastro.2020.09.020
Received 21 June 2020; Received in revised form 6 September 2020; Accepted 12 September 2020
Available online 16 September 2020

conditions, which make the methods more effective in obtaining the appropriate initial approximation solution of the low-thrust trajectory design. This kind of problem only involves the trajectory optimization between the starting planet and the arriving planet. In the calculation process, it only needs to satisfy the position and velocity constraints of the arriving planet. However, when solving the problem of fast generation of low-thrust multi gravity-assist transfer trajectories, the calculation process becomes more complex.

Different from the application of the Bezier shape-based method in the above research direction, in the low-thrust multiple gravity-assist interplanetary transfer problem studied in this paper, the spacecraft needs to accurately complete the position rendezvous with multiple gravity-assist planets in one mission, and realize gravity-assist under the corresponding constraints. Since the time-free problem is studied in this paper (the transfer time of the spacecraft between gravity-assist planets is an optimization variable), in the optimization process, the transfer time and gravity-assist effect of the spacecraft rendezvous with the previous gravity-assist planet will greatly affect the rendezvous position and fuel requirement with subsequent planets. Hence in the optimization problem of this paper, the relative position and velocity of the spacecraft and all planets should be considered simultaneously in order to obtain better transfer trajectories. Therefore, when the Bezier shape-based method is used to calculate the low-thrust multiple gravity-assist transfer trajectories, there are more variables and constraints, and the transfer process becomes more complex.

In this study, we propose a fast and effective initial approximation method for generating low-thrust multiple gravity-assist trajectories, which combines the Bezier shape-based method with the multiple gravity-assist. This study utilizes the rapidity of the Bezier shape-based method in calculating low-thrust trajectories and introduces the method into the generation process of low-thrust multiple gravity-assist trajectories. Due to the existence of multiple gravity-assist processes, the entire calculation process becomes more complex and difficult. The purpose of this study is to make the complex transfer process automatic and programmed, and finally realize the automatic and rapid acquisition of the appropriate initial approximate solution of the low-thrust multiple gravity-assist transfer trajectories under the conditions of given target stars, multiple gravity-assist stars, and launch time. In this study, four examples of the low-thrust multiple gravity-assist trajectory are presented to the Jupiter rendezvous trajectories, which are no-gravity-assist, one-gravity-assist, two-gravity-assist, and three-gravity-assist trajectories. In order to prove the effectiveness of the proposed method, the Bezier shape-based method and the FFS shape-based method are compared under the same initial conditions. At the same time, in order to verify the applicability of the results of the proposed method to the initial value of the direct optimization algorithm, the results of this paper are substituted into the GPM for further optimization, and the advantages of the proposed method are demonstrated by the comparison of the results.

This paper is organized as follows. In Section 2, dynamic equations and gravity-assist models are presented. In Section 3, the Bezier shape-based method is briefly described. In Section 4, the simulation examples and comparison results are given. Finally, in Section 5, the conclusion is given.

2. Problem description

2.1. Dynamic description

The dynamic equations of the spacecraft are established in the heliocentric coordinate system as shown in Fig. 1. The origin is at the center of mass of the sun, $x_o y_o z_o$ is the heliocentric ecliptic inertial system, and (r, θ, z) is the cylindrical coordinate system. Radial distance (r), azimuth angle (θ), and altitude (z) represent the position coordinates of the spacecraft.

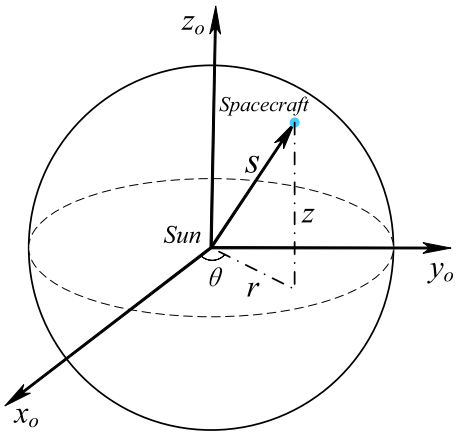

Fig. 1. Coordinate systems.

The dynamic equations of the spacecraft in the cylindrical coordinate system [30] are

$$\begin{aligned} &\ddot{r} - r\dot{\theta}^2 + \mu_\odot r/s^3 = a_r \\ &r\ddot{\theta} + 2\dot{r}\dot{\theta} = a_\theta \\ &\ddot{z} + \mu_\odot z/s^3 = a_z \end{aligned} \tag{1}$$

where $s = \sqrt{r^2 + z^2}$, $\mu_\odot$ is the gravitational parameter of the sun, and a_r, a_θ and a_z are the propulsion acceleration components. The total propulsive acceleration, (a), is

$$a = \sqrt{a_r^2 + a_\theta^2 + a_z^2} \tag{2}$$

The goal of this paper is that the spacecraft can reach the target planet with as little speed increment as possible, so the performance index is the total ΔV, which is

$$\Delta V = \int_0^T a\, dt \tag{3}$$

where T is the total flight time.

When only Earth and the target planet are considered, the following 12 boundary conditions should be met for the position and velocity.

$$\begin{aligned} &r(\tau=0) = r_{\mathrm{E}}, r(\tau=1) = r_{\mathrm{tar}}, r'(\tau=0) = T\dot{r}_{\mathrm{E}}, r'(\tau=1) = T\dot{r}_{\mathrm{tar}} \\ &\theta(\tau=0) = \theta_{\mathrm{E}}, \theta(\tau=1) = \theta_{\mathrm{tar}}, \theta'(\tau=0) = T\dot{\theta}_{\mathrm{E}}, \theta'(\tau=1) = T\dot{\theta}_{\mathrm{tar}} \\ &z(\tau=0) = z_{\mathrm{E}}, z(\tau=1) = z_{\mathrm{tar}}, z'(\tau=0) = T\dot{z}_{\mathrm{E}}, z'(\tau=1) = T\dot{z}_{\mathrm{tar}} \end{aligned} \tag{4}$$

where subscripts "E" and "tar" represent the Earth and target planet, respectively. $\tau = t/T$, where t is the flight time. The derivative with respect to time (t) and dimensionless time (τ) are denoted by the symbol $\dot{}$ and superscript $'$, respectively.

When multiple gravity-assist is considered, additional constraints need to be considered when the spacecraft approaches the gravity-assist planet. When n planets are used for gravity assistance, the entire transfer process from Earth to target planet can be divided into $n+1$ segments (each segment represents journey of the spacecraft from one planet to another), so T should also be divided into $n+1$ segments $(T_1, T_2, \ldots, T_{n+1})$. T_1 is the moment when the spacecraft approaches the first gravity-assist planet, $T_1 + T_2$ is the moment when the spacecraft approaches the second gravity-assist planet, ⋯, etc. Therefore, each time the spacecraft approaches the gravity-assist planet, the following six position conditions must be met.

$$\begin{aligned} &r(\tau\tau=0) = r_{\mathrm{PreG}}, \quad r(\tau\tau=1) = r_{\mathrm{TarG}} \\ &\theta(\tau\tau=0) = \theta_{\mathrm{PreG}}, \quad \theta(\tau\tau=1) = \theta_{\mathrm{TarG}} \\ &z(\tau\tau=0) = z_{\mathrm{PreG}}, \quad z(\tau\tau=1) = z_{\mathrm{TarG}} \end{aligned} \tag{5}$$

where $\tau\tau$ is the dimensionless time of each segment, subscript "PreG" represents the previous gravity-assist planet, and subscript "TarG" represents the target gravity-assist planet.

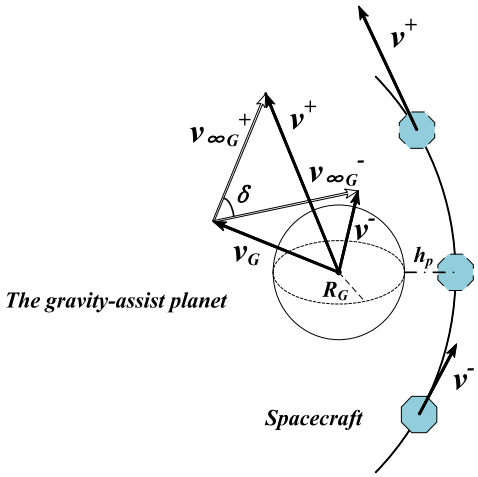

Fig. 2. Gravity-assist process.

In the process of gravity assistance, the constraint of the gravity-assist height should be considered, which should be larger than the minimum gravity-assist height of each planet ($h_p > h_{p\min}$).

2.2. Gravity-assist models

The velocity of the gravity-assist process is treated as instantaneous and discontinuous, which is caused by the instantaneous rotation of the hyperbolic velocity vector of the spacecraft relative to the gravity-assist planet. The approximate model of the linked-conic is adopted, and all disturbances are ignored. In the heliocentric coordinate system, when the position vector of the gravity-assist planet $\boldsymbol{r}_p$ is equal to that of the spacecraft $\boldsymbol{r}_S$, that is, $\boldsymbol{r}_S = \boldsymbol{r}_p$, the gravity-assist process is performed. The gravity-assist process is shown in Fig. 2.

Here the two-body equations of motion are used, and the kinematic equation is as follows,

$$\begin{aligned}
&\boldsymbol{v}_{\infty G}^{-} = \boldsymbol{v}^{-} - \boldsymbol{v}_G \\
&\boldsymbol{v}_{\infty G}^{+} = \boldsymbol{v}^{+} - \boldsymbol{v}_G \\
&\|\boldsymbol{v}_{\infty G}^{-}\| = \|\boldsymbol{v}_{\infty G}^{+}\| = v_\infty \\
&\delta = arccos\left(\frac{\boldsymbol{v}_{\infty G}^{+}\cdot\boldsymbol{v}_{\infty G}^{-}}{v_\infty^2}\right) \\
&h_p = \frac{\mu_G}{v_\infty^2}\left(\frac{1}{sin\left(\frac{\delta}{2}\right)} - 1\right) - R_G
\end{aligned} \tag{6}$$

where μ_G is the gravitational constant of the gravity-assist planet, R_G is the average radius of the gravity-assist planet, $\boldsymbol{v}_G$ is the heliocentric velocity vector of the gravity-assist planet, $\boldsymbol{v}^-$ and $\boldsymbol{v}^+$, respectively, are the heliocentric velocity vector of the spacecraft before and after the gravity assistance, $\boldsymbol{v}_{\infty G}^-$ and $\boldsymbol{v}_{\infty G}^+$, respectively, are the relative velocity of the gravity-assist planet and the spacecraft before and after the gravity assistance, v_∞ is the modulus of $\boldsymbol{v}_{\infty G}^-$ and $\boldsymbol{v}_{\infty G}^+$, and δ is the angle between $\boldsymbol{v}_{\infty G}^-$ and $\boldsymbol{v}_{\infty G}^+$.

3. Bezier shape-based method

3.1. States approximation

Based on Ref. [34,35], the coordinates of the spacecraft are expressed in the form of the Bezier method, and coordinate r is taken as an example.

$$r(\tau) = \sum_{j=0}^{n_r} B_{r,j}(\tau)P_{r,j} \tag{7}$$

where n_r is the order of Bezier function, and $P_{r,j}$ are the unknown Bezier coefficients.

$$B_{r,j}(\tau) = \frac{n_r!}{j!(n_r-j)!}\tau^j(1-\tau)^{n_r-j} \qquad j \in [0, n_r] \tag{8}$$

The first-order and second-order τ-derivatives are

$$r'(\tau) = \sum_{j=0}^{n_r} B'_{r,j}(\tau)P_{r,j} \qquad r''(\tau) = \sum_{j=0}^{n_r} B''_{r,j}(\tau)P_{r,j} \tag{9}$$

where the specific forms of $B'_{r,j}(\tau)$ and $B''_{r,j}(\tau)$ can be found in Ref. [34]. When $\tau = 0$ and $\tau = 1$, we can obtain

$$\begin{aligned}
&B_{r,j}(\tau=0) = \begin{cases} 1 & j = 0 \\ 0 & j \in [1, n_r] \end{cases} \quad B_{r,j}(\tau=1) = \begin{cases} 0 & j \in [0, n_r-1] \\ 1 & j = n_r \end{cases} \\
&B'_{r,j}(\tau=0) = \begin{cases} -n_r & j = 0 \\ n_r & j = 1 \\ 0 & j \in [2, n_r] \end{cases} \quad B'_{r,j}(\tau=1) = \begin{cases} 0 & j \in [0, n_r-2] \\ -n_r & j = n_r-1 \\ n_r & j = n_r \end{cases}
\end{aligned} \tag{10}$$

Therefore, by the constraint of boundary conditions in Eq. (4), we can obtain

$$\begin{aligned}
&r_{\mathrm{E}} = r(\tau=0) = P_{r,0} \\
&r_{\mathrm{tar}} = r(\tau=1) = P_{r,n_r} \\
&T\dot{r}_{\mathrm{E}} = r'(\tau=0) = n_r(P_{r,1} - P_{r,0}) \\
&T\dot{r}_{\mathrm{tar}} = r'(\tau=1) = n_r(P_{r,n_r} - P_{r,n_r-1})
\end{aligned} \tag{11}$$

Consequently, $P_{r,0}$, $P_{r,1}$, P_{r,n_r-1}, and P_{r,n_r} can be acquired

$$\begin{aligned}
&P_{r,0} = r_{\mathrm{E}} \qquad P_{r,1} = r_{\mathrm{E}} + T\dot{r}_{\mathrm{E}}/n_r \\
&P_{r,n_r-1} = r_{\mathrm{tar}} - T\dot{r}_{\mathrm{tar}}/n_r \qquad P_{r,n_r} = r_{\mathrm{tar}}
\end{aligned} \tag{12}$$

Through the discretization of τ, which uses the Legendre–Gauss distribution of discrete points (the roots of the mth-degree Legendre polynomial), the transfer trajectory is constrained.

$$\tau_1 = 0 < \tau_2 < \cdots < \tau_{m-1} < \tau_m = 1 \tag{13}$$

Therefore, r and its derivatives are expressed in matrix form,

$$\begin{aligned}
&[r]_{m\times 1} = [B_r]_{m\times(n_r+1)}[P_r]_{(n_r+1)\times 1} \\
&[r']_{m\times 1} = [B'_r]_{m\times(n_r+1)}[P_r]_{(n_r+1)\times 1} \\
&[r'']_{m\times 1} = [B''_r]_{m\times(n_r+1)}[P_r]_{(n_r+1)\times 1}
\end{aligned} \tag{14}$$

where $[P_r] = \begin{bmatrix} P_{r,0} & P_{r,1} & [X_r]^T_{(n_r-3)\times 1} & P_{r,n_r-1} & P_{r,n_r} \end{bmatrix}^T$, and $[B_r]$, $[B'_r]$, $[B''_r]$ can be computed by n_r and discrete points. $[X_r]_{(n_r-3)\times 1} = \begin{bmatrix} P_{r,2} & \cdots & P_{r,n_r-2} \end{bmatrix}^T$ are the unknown coefficients.

a_r, a_θ, and a_z are expressed in a matrix form,

$$\begin{aligned}
&[a_r]_{m\times 1} = a_r\left([r]_{m\times 1}, [z]_{m\times 1}, [\theta']_{m\times 1}, [r'']_{m\times 1}\right) \\
&[a_\theta]_{m\times 1} = a_\theta\left([r]_{m\times 1}, [r']_{m\times 1}, [\theta']_{m\times 1}, [\theta'']_{m\times 1}\right) \\
&[a_z]_{m\times 1} = a_z\left([r]_{m\times 1}, [z]_{m\times 1}, [z'']_{m\times 1}\right)
\end{aligned} \tag{15}$$

and

$$[a] = \sqrt{[a_r]^2 + [a_\theta]^2 + [a_z]^2} \tag{16}$$

Hence, the problem in this paper can be transformed into nonlinear programming problem

$$\begin{aligned}
&\min_{[X_r],[X_\theta],[X_z],T_1,\ldots,T_{n+1},h_{p1},\ldots,h_{pn},\boldsymbol{v}_1^-,\ldots,\boldsymbol{v}_n^-} \quad \Delta V \\
&\text{s.t.} \quad [a] \le a_{\max}
\end{aligned} \tag{17}$$

where $[X_r]_{(n_r-3)\times 1}$, $[X_\theta]_{(n_\theta-3)\times 1}$, $[X_z]_{(n_z-3)\times 1}$ are the unknown Bezier coefficients, $a_{\max}$ is the maximum value of a, $h_{p1}, \ldots, h_{pn}$ are the gravity-assist height of each planet, and $\boldsymbol{v}_1^-, \ldots, \boldsymbol{v}_n^-$ are the velocity of the spacecraft as it enters the sphere of influence of each gravity-assist planet.

3.2. Initialization of unknown coefficients

In the process of iterative optimization, it is necessary to select the appropriate initial value, and subscript "APP" represents the appropriate initial value. $h_{p_{APP}} = 2h_{pmin}$. The problem studied in this paper is the time-free problem. The transfer time of the spacecraft between gravity-assist planets is an optimization variable, which needs to be solved iteratively in the calculation process. Initialization of the values of the flight time along each trajectory leg is as follows: assuming that the orbits of the planets are circular and coplanar, double pulse transfer is used to calculate T_{APP}.

$$T_{APP} = \frac{\left|\sqrt{\frac{\mu_\odot}{R_2}}\left[\sqrt{\frac{2R_1}{R_1+R_2}}\left(1-\frac{R_2}{R_1}\right)+\sqrt{\frac{R_2}{R_1}}-1\right]\right|}{a_{\max}} \times 2 \quad R_1 \neq R_2 \tag{18}$$

where R_1 and R_2 are the orbital semimajor axes of the two adjacent planets during spacecraft planetary transfer, respectively. When $R_1 = R_2$, T_{APP} is the orbital period of the planet. To reduce the gap between T_{APP} and T, multiply the result by 2.

When the order of the Bezier curve is 3, all coefficients of the Bezier curve can be determined by Eqs. (7), (8), (10), (11) and (12). When the order of Bezier curve is greater than 3, the unknown coefficients of the Bezier curve need to be optimized. Therefore, this paper uses $n_r = n_\theta = n_z = 3$ to initialize r, θ, and z, as follows:

$$r_{APP}(\tau) = (1-\tau)^3 P_{r,0} + 3\tau(1-\tau)^2 P_{r,1} + 3\tau^2(1-\tau)P_{r,2} + \tau^3 P_{r,3} \tag{19}$$

and

$$\begin{aligned} P_{r,0} &= r_E & P_{r,1} &= r_E + T_{APP}\dot{r}_E/3 \\ P_{r,2} &= r_{tar} - T_{APP}\dot{r}_{tar}/3 & P_{r,3} &= r_{tar} \end{aligned} \tag{20}$$

For $\boldsymbol{v}_1^-, \ldots, \boldsymbol{v}_n^-$, the initial value should also be given,

$$\boldsymbol{v}_{n_{APP}}^- = 0.8 \cdot \boldsymbol{v}_{Gn} + \varepsilon \tag{21}$$

where $\boldsymbol{v}_{Gn}$ is the velocity of the nth gravity-assist planet, and ε is a small value of velocity.

4. Numerical simulations

As the largest planetary system in the solar system, the Jupiter system is of great scientific value and the focus of various studies. Therefore, the final target in this paper is Jupiter and four examples of low-thrust multiple gravity-assist trajectories are presented to the Jupiter rendezvous trajectories. To reflect the effect of the gravity assist, the first example does not use gravity assist, which is compared with the following three examples. The launch date is represented by the modified Julian date (MJD). To obtain a more suitable launch date and verify the effectiveness of the proposed method, the launch date of each example is traversed between 61420 and 63382, and the traversal interval is 2 days. The orders of Bezier function are $n_r = 12$, $n_\theta = 12$, and $n_z = 16$. $m = 120$ and $a_{\max} = 1.5\times10^{-4}\mathrm{m/s^2}$ [30]. All examples were studied on a Core i5 2.50 GHz processor with Windows 10 and run on MATLAB R2015b. When the Bezier method and the FFS method are used to solve the problem, the NLP in Eq. (17) is solved by using the interior point method; when the GPM is used to solve the problem, the NLP is solved by sequential quadratic programming (SQP). The interior point method and SQP are both implemented by using the MATLAB function "fmincon".

4.1. No-gravity-assist: Earth–Jupiter

For the transfer trajectory from Earth to Jupiter without gravity assistance, the traversal results of the launch date are shown in Fig. 3. The blue circle in the figure shows the performance index under the corresponding launch date, and 351 feasible solutions have been obtained. The red dot indicates the best result in the traversal results,

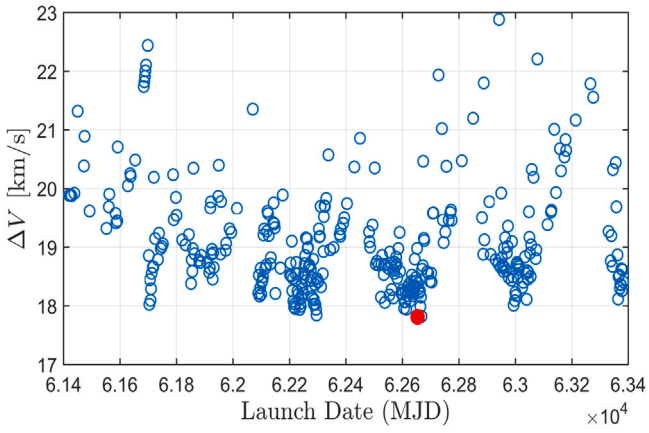

Fig. 3. Traversal results of Earth–Jupiter launch date. (For interpretation of the references to color in this figure legend, the reader is referred to the web version of this article.)

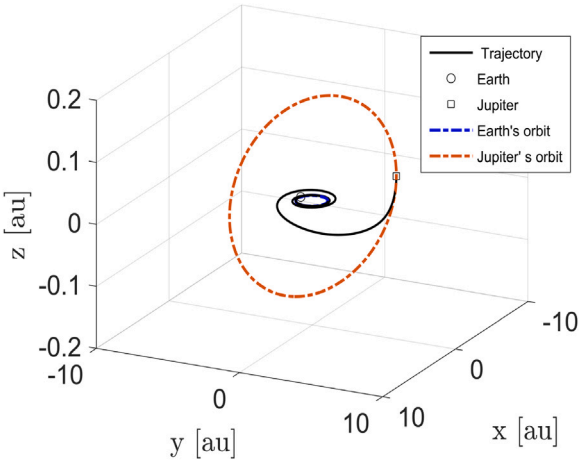

Fig. 4. Transfer trajectory of Earth–Jupiter.

and the corresponding launch date is MJD = 62654. As can be seen from Fig. 3, the feasible launch date will appear periodically, within a period of approximately 400 days.

Through the above traversal results of the launch window, the current optimal launch date is obtained, so the launch date is taken as the input launch window of this example. Therefore, the three-dimensional transfer trajectory from Earth to Jupiter is shown in Fig. 4, and the propulsive acceleration and its components in this process are shown in Fig. 5. The performance index, ΔV, of the transfer process is 17.81 km/s, and the transfer time is 2863.6 days. It can be seen from Fig. 5 that the propulsive acceleration can meet the corresponding constraints. The computation time is 18.11 s.

4.2. One-gravity-assist: Earth–Mars–Jupiter

For the transfer trajectory from Earth to Jupiter using Mars gravity assistance, the traversal results of the launch date are shown in Fig. 6. The blue circles represent the feasible solutions, and 428 feasible solutions are obtained. The red circle represents the current optimal launch date, which is MJD = 61872. According to Fig. 6, the feasible launch date will appear periodically, within a period of approximately 800 days.

When the launch date is MJD = 61872, the three-dimensional transfer trajectory from the Earth to Jupiter using Mars gravity assistance (Earth–Mars–Jupiter) is shown in Fig. 7, and the propulsive

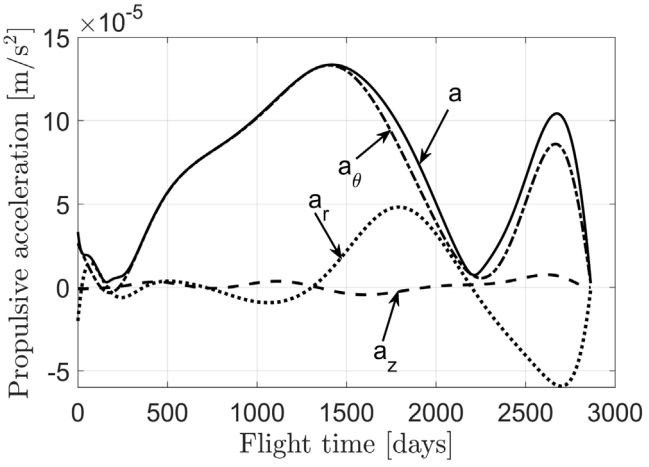

Fig. 5. Propulsive acceleration of the Earth–Jupiter transfer trajectory.

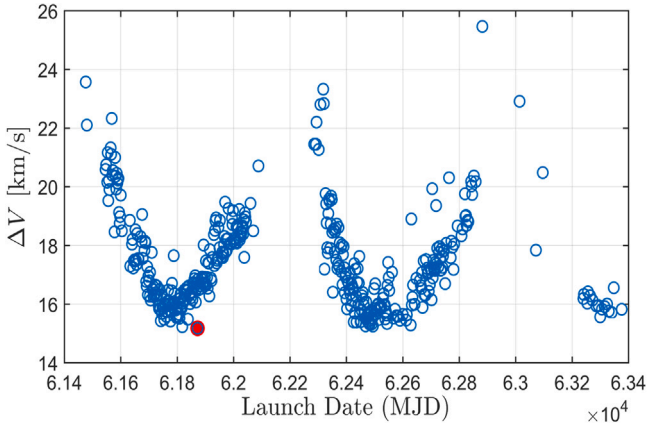

Fig. 6. Traversal results of Earth–Mars–Jupiter launch date. (For interpretation of the references to color in this figure legend, the reader is referred to the web version of this article.)

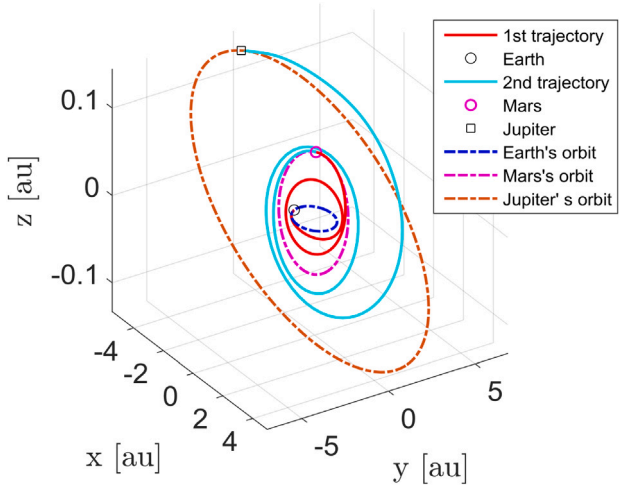

Fig. 7. Transfer trajectory of Earth–Mars–Jupiter.

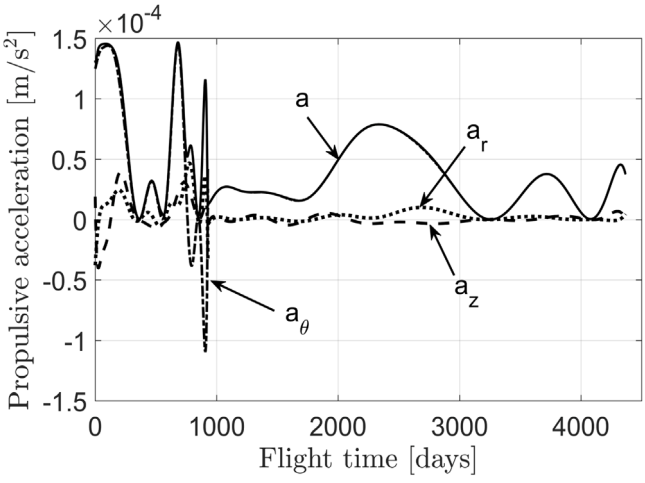

Fig. 8. Propulsive acceleration of the Earth–Mars–Jupiter transfer trajectory.

acceleration and its components in this process are shown in Fig. 8. The performance index of the transfer process is ΔV = 15.18 km/s, and the transfer time is 4366.7 days. According to Fig. 8, the propulsive acceleration can meet the corresponding constraints. The computation time is 24.21 s.

4.3. Two-gravity-assist: Earth–Earth–Mars–Jupiter

For the transfer trajectory from Earth to Jupiter using Earth and Mars gravity assistance, the traversal results of the launch date are shown in Fig. 9. There are 312 feasible solutions. The current optimal launch date is MJD = 61452. According to Fig. 9, the feasible launch date will appear periodically, within a period of approximately 800 days.

When the launch date is MJD = 61452, the three-dimensional transfer trajectory from Earth to Jupiter using Earth and Mars gravity assistance (Earth–Earth–Mars–Jupiter) is shown in Fig. 10, and the propulsive acceleration and its components are shown in Fig. 11. The performance index is ΔV = 14.95 km/s, and the transfer time is 4653.9 days. It can be seen from Fig. 11 that the propulsive acceleration can meet the corresponding constraints. The computation time is 52.59 s.

4.4. Three-gravity-assist: Earth–Earth–Earth–Mars–Jupiter

For gravity-assist transfer trajectory from Earth to Jupiter using Earth, Earth, and Mars, the traversal results of the launch date are

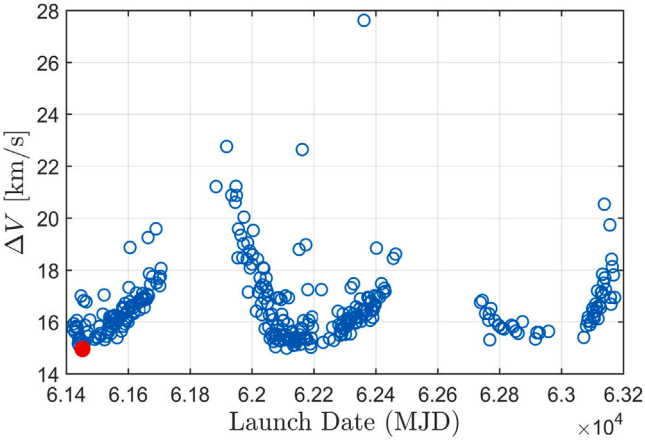

Fig. 9. Traversal results of Earth–Earth–Mars–Jupiter launch date.

shown in Fig. 12. There are 192 feasible solutions. The current optimal launch date is MJD = 61872. According to Fig. 12, the feasible launch date will also appear periodically, within a period of approximately 800 days.

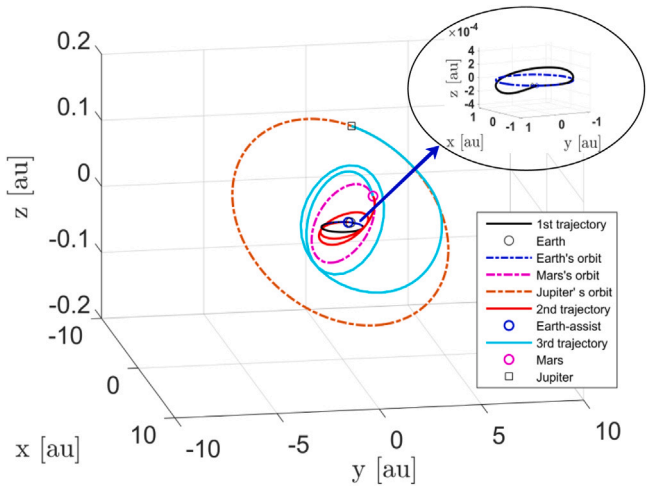

Fig. 10. Transfer trajectory of Earth–Earth–Mars–Jupiter.

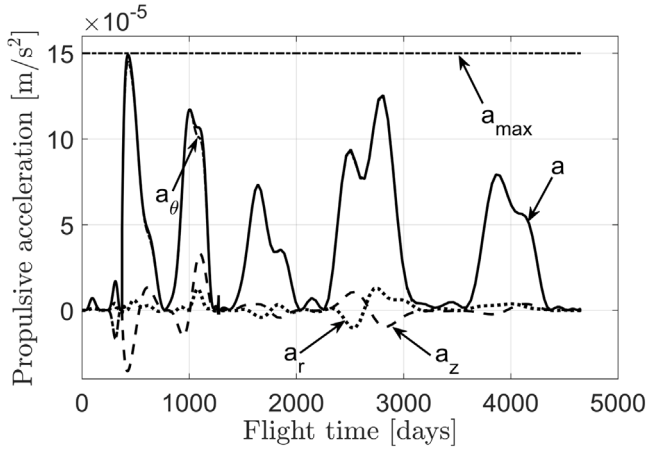

Fig. 11. Propulsive acceleration of the Earth–Earth–Mars–Jupiter transfer trajectory.

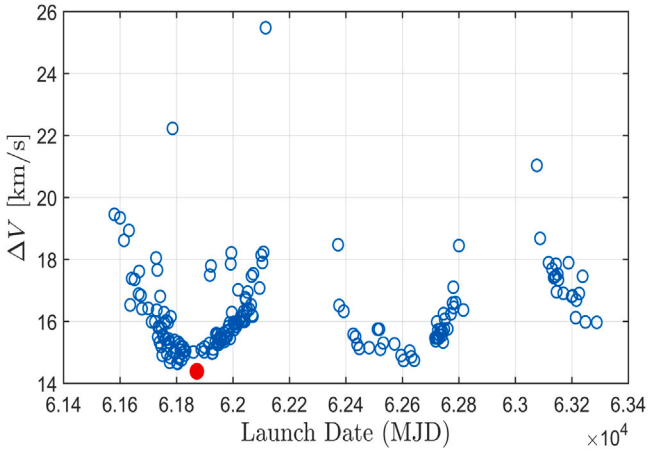

Fig. 12. Traversal results of Earth–Earth–Earth–Mars–Jupiter launch date.

When the launch date is MJD = 61872, the three-dimensional gravity-assist transfer trajectory from Earth to Jupiter using Earth, Earth, and Mars (Earth–Earth–Earth–Mars–Jupiter) is shown in Fig. 13, and the propulsive acceleration and its components are shown in Fig. 14. The performance index is ΔV = 14.39 km/s, the transfer time is 3432.2 days, and the computation time is 96.47 s.

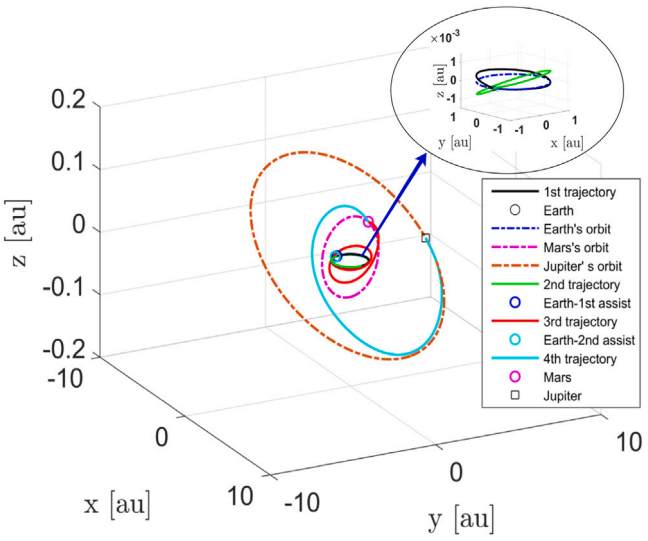

Fig. 13. Transfer trajectory of Earth–Earth–Earth–Mars–Jupiter.

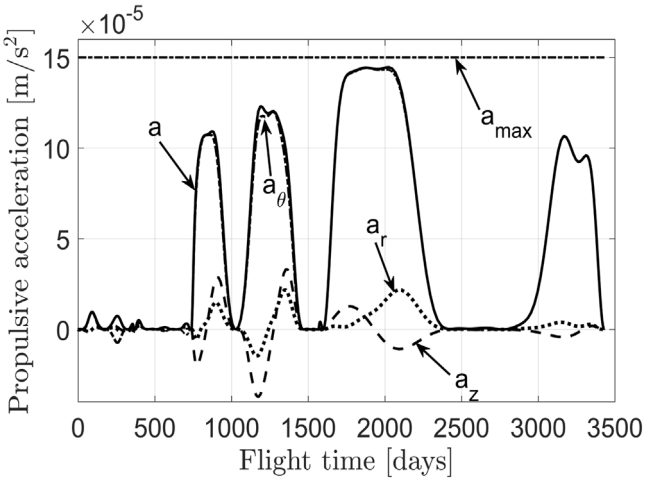

Fig. 14. Propulsive acceleration of the Earth–Earth–Earth–Mars–Jupiter transfer trajectory.

4.5. Results comparison

The results of the above four examples are shown in Table 1. Firstly, the results obtained by using the Bezier shape-based method in four simulation examples are analyzed. Compared with the results of no-gravity-assist, the performance index of one-gravity-assist is reduced by 2.63 km/s. In the same range of launch dates, there are more feasible solutions, but the transfer time is increased by 1503.1 days, and the computation time is increased by 6.10 s. Compared with one-gravity-assist, the performance index of two-gravity-assist is further reduced by 0.23 km/s, but in the same range of launch dates, the number of feasible solutions is reduced by 116, the transfer time is increased by 287.2 days, and the computation time is increased by 28.38 s. When comparing the results of three-gravity-assist and two-gravity-assist, the performance index of three-gravity-assist is reduced by 0.56 km/s, and the transfer time is reduced by 1221.7 days. However, in the same range of launch dates, the number of feasible solutions is reduced by 120, and the computation time is increased by 43.88 s.

Then, under the same initial conditions, the Bezier shape-based method is compared with the FFS shape-based method. Through the comparison of the results obtained by the two methods in Table 1, it

Table 1
Comparison of the Bezier shape-based method, the FFS shape-based method and the GPM.

Transfer process	Launch date (MJD)	ΔV/(km/s)			Computation time/(s)			T/(day)		Δv by gravity-assist[a]/(km/s)		Feasible solutions by Bezier
		Bezier	FFS	GPM	Bezier	FFS	GPM	Bezier	FFS	Bezier	FFS	
No-gravity-assist: Earth–Jupiter	62 654	17.81	17.90	17.49	18.11	20.63	1767.6	2863.6	3646.5	–	–	351
One-gravity-assist: Earth–Mars–Jupiter	61 872	15.18	16.98	14.83	24.21	37.74	2129.7	4366.7	4375.6	2.84	2.44	428
Two-gravity-assist: Earth–Earth–Mars–Jupiter	61 452	14.95	16.30	14.85	52.59	92.25	2563.5	4653.9	4026.9	0.20 2.01	0.58 2.07	312
Three-gravity-assist: Earth–Earth–Earth–Mars–Jupiter	61 872	14.39	15.92	14.32	96.47	188.26	3449.6	3432.2	3433.6	0.32 0.30 3.49	1.00 0.84 2.91	192

[a]"Δv by Gravity-Assist" is the velocity increment obtained by the spacecraft after each gravity assist.

can be seen that in the four simulation examples, the Bezier shape-based method can use shorter computation time to obtain the transfer trajectories, and the velocity increment required by the Bezier shape-based method in the transfer process is also less. Moreover, with the increase of the number of gravity-assist planets, the difference in computation time becomes larger.

Finally, in order to verify the applicability of the results of the proposed method to the initial value of the direct optimization algorithm, the results of this paper are substituted into GPM as the initial value for further optimization. Through the comparison of the results obtained by the two methods in Table 1, it can be seen that although the results obtained by the Bezier method are used as the initial values, the difference between the performance indexes of the Bezier method and GPM is only about 2%, while the Bezier method only uses approximately 2% of the computation time of the GPM. Therefore, the method described in this paper is of great significance to quickly obtain the feasible initial solutions of a large number of design examples.

5. Conclusion

In this study, a fast initial design method of low-thrust trajectory is proposed, which combines low-thrust propulsion and multiple gravity-assist technology. This paper combines the Bezier shape-based method with the gravity-assist algorithm to obtain a fast algorithm for calculating the low-thrust multiple gravity-assist transfer trajectories. To design Jupiter rendezvous trajectories, the feasibility of the proposed method are proved by comparing four examples, which are no-gravity-assist, one-gravity-assist, two-gravity-assist, and three-gravity-assist trajectories. Compared with the results of no-gravity-assist, the performance index of three-gravity-assist is reduced by 3.42 km/s, and the transfer time is only increased by 568.6 days. The computation time of the three-gravity-assist example is 96.47 s. In order to verify the effectiveness of the proposed method, the Bezier shape-based method and the FFS shape-based method are compared under the same initial conditions. The simulation results show that compared with the FFS shape-based method, the proposed method can obtain transfer trajectories with smaller velocity increments in shorter computation time. In order to verify the applicability of the results of the method proposed in this paper to the initial value of the direct optimization algorithm, the results of this paper are substituted into the GPM as the initial value for further optimization. The Bezier method only uses approximately 2% of the computation time of the GPM to obtain the results that are only about 2% different from the performance index of the GPM. For a large number of gravity-assist design cases, the method described in this paper is crucial for acquiring a feasible initial solution quickly.

In the simulation examples in this paper, the selection of gravity-assist planets and the determination of gravity-assist sequences are based on the previous references and some simulation experiments. The future research direction is how to quickly and accurately select the optimal gravity-assist stars and corresponding flying sequences from a large number of gravity-assist stars.

Declaration of competing interest

The authors declare that they have no known competing financial interests or personal relationships that could have appeared to influence the work reported in this paper.

Acknowledgment

This work is supported by the National Natural Science Foundation of China under Grant Nos. U1737207 and 11672093.

References

[1] T. Wen, X. Zeng, C. Circi, Y. Gao, Hop reachable domain on irregularly shaped asteroids, J. Guid. Control Dyn. 43 (7) (2020) 1269–1283.
[2] Y. Zhang, X. Zeng, F. Zhang, Spacecraft hovering flight in a binary asteroid system by using fuzzy logic control, IEEE Trans. Aerosp. Electron. Syst. 55 (6) (2019) 3246–3258.
[3] B. Yang, H. Yang, S. Li, Pseudostate theory based iterative preliminary design method for powered gravity-assist interplanetary trajectories, Acta Astronaut. 165 (2019) 139–149.
[4] D. Tamakoshi, H. Kojima, Set-oriented design of interplanetary low-thrust trajectories using Earth Gravity Assist, Acta Astronaut. 156 (2019) 208–218.
[5] Y. Lu, S.J. Saikia, Titan aerogravity-assist maneuvers for Saturn/Enceladus missions, Acta Astronaut. 176 (2020) 262–275.
[6] S. Lee, I. Hwang, Reachable set computation for spacecraft relative motion with energy-limited low-thrust, Aerosp. Sci. Technol. 77 (2018) 180–188.
[7] A. Weiss, U.V. Kalabić, S.D. Cairano, Station keeping and momentum management of low-thrust satellites using MPC, Aerosp. Sci. Technol. 76 (2018) 229–241.
[8] M.D. Rayman, P. Varghese, D.H. Lehman, L.L. Livesay, Results from the Deep Space 1 technology validation mission, Acta Astronaut. 47 (2–9) (2000) 475–487.
[9] M.D. Rayman, S.N. Williams, Design of the first interplanetary solar electric propulsion mission, J. Spacecr. Rockets 39 (4) (2002) 589–595.
[10] M.B. Murrill, The grandest tour: VOYAGER, Mercury 22 (3) (1993) 66–77.
[11] M. Vasile, P. De Pascale, Preliminary design of multiple gravity-assist trajectories, J. Spacecr. Rockets 43 (4) (2006) 794–805.
[12] S.N. Williams, V. Coverstone-Carroll, Benefits of solar electric propulsion for the next generation of planetary exploration missions, J. Astronaut. Sci. 45 (2) (1997) 143–159.
[13] C.A. Kluever, M. Abu-Saymeh, Mercury mission design using solar electric propulsion, J. Spacecr. Rockets 35 (3) (1998) 411–413.
[14] Y. Langevin, Chemical and solar electric propulsion options for a mercury cornerstone mission, Acta Astronaut. 47 (2) (2000) 443–452.
[15] M. Macdonald, C.R. McInnes, Spacecraft planetary capture using gravity-assist maneuvers, J. Guid. Control Dyn. 28 (2) (2005) 365–368.
[16] O. Schütze, M. Vasile, O. Junge, M. Dellnitz, D. Izzo, Designing optimal low-thrust gravity-assist trajectories using space pruning and a multiobjective approach, Eng. Optim. 41 (2) (2009) 155–181.

[17] D. Benson, A Gauss Pseudospectral Transcription for Optimal Control (Ph.D. thesis), Department of Aeronautics and Astronautics, MIT, 2004.
[18] A.E. Petropoulos, J.M. Longuski, Shape-based algorithm for automated design of low-thrust, gravity-assist trajectories, J. Spacecr. Rockets 41 (5) (2004) 787–796.
[19] P. De Pascale, M. Vasile, Preliminary design of low-thrust multiple gravity-assist trajectories, J. Spacecr. Rockets 43 (5) (2006) 1069–1076.
[20] B.J. Wall, B.A. Conway, Shape-Based approach to low-thrust rendezvous trajectory design, J. Guid. Control Dyn. 32 (1) (2009) 95–101.
[21] B. Wall, Shape-based approximation method for low-thrust trajectory optimization, in: AIAA/AAS Astrodynamics Specialist Conference and Exhibit., 2008, pp. 2008–6616.
[22] D.M. Novak, M. Vasile, Improved shaping approach to the preliminary design of low-thrust trajectories, J. Guid. Control Dyn. 34 (1) (2011) 128–147.
[23] C. Xie, G. Zhang, Y. Zhang, Simple shaping approximation for low-thrust trajectories between coplanar elliptical orbits, J. Guid. Control Dyn. 38 (12) (2015) 2448–2455.
[24] D.J. Gondelach, R. Noomen, Hodographic-shaping method for low-thrust interplanetary trajectory design, J. Spacecr. Rockets 52 (3) (2015) 728–738.
[25] C. Xie, G. Zhang, Y. Zhang, Shaping approximation for low-thrust trajectories with large out-of-plane motion, J. Guid. Control Dyn. 39 (12) (2016).
[26] K. Zeng, Y. Geng, B. Wu, Shape-based analytic safe trajectory design for spacecraft equipped with low-thrust engines, Aerosp. Sci. Technol. 62 (2017) 87–97.
[27] A. Peloni, B. Dachwald, M. Ceriotti, Multiple near-earth asteroid rendezvous mission: Solar-sailing options, Adv. Space Res. 62 (8) (2018) 2084–2098.
[28] O. Abdelkhalik, E. Taheri, Approximate on-off low-thrust space trajectories using Fourier series, J. Spacecr. Rockets 49 (5) (2012) 962–965.
[29] E. Taheri, O. Abdelkhalik, Fast initial trajectory design for low-thrust restricted-three-body problems, J. Guid. Control Dyn. 38 (11) (2015) 1–15.
[30] E. Taheri, O. Abdelkhalik, Initial three-dimensional low-thrust trajectory design, Adv. Space Res. 57 (3) (2016) 889–903.
[31] E. Taheri, I. Kolmanovsky, E. Atkins, Shaping low-thrust trajectories with thrust-handling feature, Adv. Space Res. 61 (3) (2018) 879–890.
[32] M. Huo, G. Zhang, N. Qi, Y. Liu, X. Shi, Initial trajectory design of electric solar wind sail based on finite Fourier series shape-based method, IEEE Trans. Aerosp. Electron. Syst. 55 (6) (2019) 3674–3683.
[33] Z. Fan, M. Huo, N. Qi, Y. Xu, Z. Song, Fast preliminary design of low-thrust trajectories for multi-asteroid exploration, Aerosp. Sci. Technol. 93 (2019).
[34] M. Huo, G. Mengali, A. Quarta, N. Qi, Electric sail trajectory design with Bezier curve-based shaping approach, Aerosp. Sci. Technol. 88 (2019) 126–135.
[35] Z. Fan, M. Huo, N. Qi, C. Zhao, Z. Yu, T. Lin, Initial design of low-thrust trajectories based on the Bezier curve-based shaping approach, Proc. Inst. Mech. Eng. G (2020) http://dx.doi.org/10.1177/0954410020920040.